

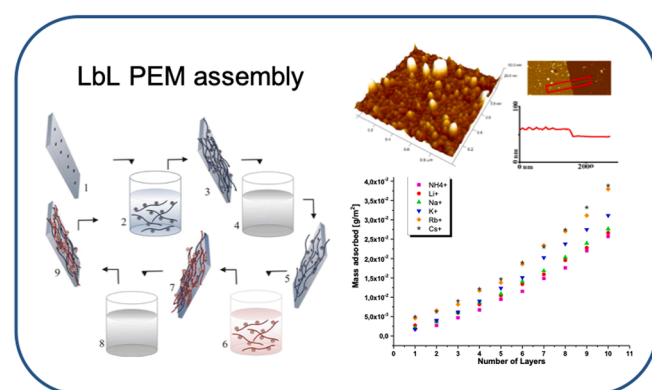
# Specific ion effects on the build-up and permeability of poly(diallyldimethylammonium) chloride/poly(sodium 4-styrenesulfonate) polyelectrolyte multilayers

Marta Kolasinska-Sojka<sup>a,\*</sup>, Magdalena Wlodek<sup>a</sup>, Michal Szuwarzynski<sup>b</sup>, Piotr Warszynski<sup>a</sup>

<sup>a</sup> Jerzy Haber Institute of Catalysis and Surface Chemistry, Polish Academy of Sciences, Niezapominajek 8, Krakow PL-30239, Poland

<sup>b</sup> AGH University of Krakow, Academic Centre for Materials and Nanotechnology, al. A. Mickiewicza 30, Krakow PL-30059, Poland

## GRAPHICAL ABSTRACT



## ARTICLE INFO

### Keywords:

Ion specific interactions  
Multilayer permeability  
Polyelectrolyte multilayers

## ABSTRACT

Polyelectrolyte multilayers (PEMs) are very promising systems in the field of material science, intensively developed and broadly examined with constantly increasing interest in applications such as sensors, coatings, membranes, and biomedical interfaces. While the impact of ionic strength on PEM formation is well established, the influence of specific counterions remains underexplored. In this study, we systematically examine the effect of six monovalent cations— $\text{NH}_4^+$ ,  $\text{Li}^+$ ,  $\text{Na}^+$ ,  $\text{K}^+$ ,  $\text{Rb}^+$ , and  $\text{Cs}^+$ —on the build-up, morphology, permeability, and surface wettability of PDADMAC/PSS multilayers assembled via the layer-by-layer technique. Using a combination of quartz crystal microbalance with dissipation (QCM-D), atomic force microscopy (AFM), cyclic voltammetry, and contact angle measurements, we demonstrate that the physicochemical properties of PEMs are strongly influenced by cation identity. Larger, chaotropic cations ( $\text{Rb}^+$ ,  $\text{Cs}^+$ ) produce thicker, smoother, and more compact films with reduced permeability, consistent with enhanced charge screening and interchain packing. In contrast, smaller, kosmotropic cations ( $\text{Li}^+$ ,  $\text{Na}^+$ ) lead to thinner, rougher, and more permeable films, suggesting weaker chain interactions and looser film structures.  $\text{K}^+$  induces exceptionally high surface hydrophobicity and blocking efficiency, while  $\text{NH}_4^+$  shows distinct behavior likely due to its hydrogen-bonding capabilities. A clear

\* Corresponding author.

E-mail address: [marta.kolasinska-sojka@ikifp.edu.pl](mailto:marta.kolasinska-sojka@ikifp.edu.pl) (M. Kolasinska-Sojka).

<https://doi.org/10.1016/j.colsurfa.2025.137681>

Received 17 March 2025; Received in revised form 7 May 2025; Accepted 4 July 2025

Available online 5 July 2025

0927-7757/© 2025 The Authors. Published by Elsevier B.V. This is an open access article under the CC BY license (<http://creativecommons.org/licenses/by/4.0/>).

odd–even alternation in contact angle was observed, driven by the chemical nature of the terminating layer (PDADMAC vs. PSS), highlighting the importance of surface composition in wetting behavior. These findings demonstrate that even subtle differences in ion type can modulate film growth kinetics, surface morphology, and functional performance. The results offer new insights into the design of PEMs with tailored permeability, roughness, and surface energy, with direct implications for their optimization in electrochemical sensors, anti-fouling coatings, and controlled-release systems.

## 1. Introduction

Polyelectrolyte multilayers (PEM), assembled by the Layer-by-Layer technique (LbL) [1,2] have been established an fundamental platform in interface science and engineering proving their position in the wide world of applications [3–7]. Their rapid development and interest for practical use in fields such as sensors, membranes, coatings or drug delivery is own to tunable physicochemical properties and versatile capacity over precise control of their structure and functionality [8–12]. As far as tuning is concerned, one has to know that PEMs are influenced by number of factors such as the type of polyelectrolyte, deposition conditions, i.e., ionic strength and pH value [13–15], as well as the nature of counterions. The influence of ions during the assembly process is of fundamental significance. Both the ionic strength and the distinct properties of the ions themselves are crucial in modulation of the films' thickness, permeability, and mechanical features of the multilayer structure [16,17]. The Hofmeister series [18], originally developed to explain how ions affect protein solubility and stability [19], offers a useful model for interpreting ion-specific interactions in polyelectrolyte systems [20–23]. It classifies ions according to their chaotropic (disorder-promoting) or kosmotropic (order-promoting) tendencies. Typically, the Hofmeister series for cations is arranged as  $\text{Cs}^+ > \text{Rb}^+ > \text{K}^+ > \text{Na}^+ > \text{Li}^+$ , reflecting a progression from chaotropic (structure-breaking) to kosmotropic (structure-making) [24].  $\text{NH}_4^+$  often deviates from this pattern, exhibiting anomalous behavior due to its higher hydrogen-bonding capability [24]. Smaller, kosmotropic ions, such as  $\text{Li}^+$ , with robust hydration shells, tend to foster ordered yet thinner films, whereas larger, chaotropic ions, like  $\text{Cs}^+$ , with weaker hydration, promote the formation of thicker and potentially more disordered structures [25]. Such ion-specific effects are particularly significant in polyelectrolyte multilayers, where counterions mediate the interchain interactions, packing and conformation of polyions throughout the LbL process [26–28]. It is meaningful in controlled release systems [29], in sensor technology to enable selectivity to electrochemical probes or optical signal [30]. PEMs applied as coatings provide corrosion resistance and/or biocompatibility for medical implants [31], while serving as membranes they support water purification or fuel cells [32]. The ability to customize PEM properties and functionality through the selection of counterions is therefore crucial for tailoring these applications. Thus, a deeper understanding of ion-specific effects is essential. Despite advances in the field, the precise mechanisms by which Hofmeister series cations influence the buildup, surface characteristics and permeability of PEMs remain incompletely elucidated. To bridge this gap, the present work investigates the influence of monovalent counter-cations ( $\text{NH}_4^+$ ,  $\text{Li}^+$ ,  $\text{Na}^+$ ,  $\text{K}^+$ ,  $\text{Rb}^+$ ,  $\text{Cs}^+$ ) on the assembly and properties of poly(diallyldimethylammonium) chloride (PDADMAC) and poly(sodium 4-styrenesulfonate) (PSS) multilayers. Using quartz crystal microbalance with dissipation (QCM-D), we studied film growth and viscoelastic responses under *in situ* deposition in dependence on selected counter-cations. Electrochemical measurements revealed permeability for redox probes while atomic force microscopy (AFM) provided topographical and roughness information. Complementary contact-angle experiments elucidated how cation-specific structures manifest in altered wetting characteristics. By systematically correlating these structural and functional data, this study advances our understanding of how Hofmeister effects can fine-tune PEM properties. Such insights may guide the rational design of multifunctional coatings.

## 2. Materials and methods

### 2.1. Materials and sample preparation

The polyelectrolytes applied in the current studies were: poly(diallyldimethylammonium) chloride (PDADMAC) with the molecular weight in the range of 100–200 kDa as *polycation*, and polysodium 4-styrenesulfonate (PSS) of 70 kDa as *polyanion*, both purchased from Sigma-Aldrich. Silicon wafers with orientation  $100^\circ \pm 0.5^\circ$  (On Semi-conductor, Czech Republic) were used as support for multilayers for AFM and wetting characteristics, standard gold/quartz sensors QSX 301 (Q-Sense, Sweden) were applied for QCM studies. They both were cleaned with piranha solution - equivalent volumes' mixture of concentrated sulfuric acid and perhydrol (*Precaution! This solution is a very strong oxidizing agent and should be handled carefully under the hood*) then rinsed with Millipore water and soaked for 30 min in hot water ( $70^\circ \text{C}$ ). For cyclic voltammetry PEM were deposited on the gold disk electrodes applied as working electrodes. Before use gold electrodes were polished using aluminium oxide ( $\text{Al}_2\text{O}_3$ ,  $\phi = 0.05 \mu\text{m}$ , Buehler, Switzerland) and cycled in 0.1 M  $\text{HClO}_4$  in the potential range from 0.2 to 1.5 V vs. Ag/AgCl/KCl(saturated) at the scan rate of  $100 \text{ mV s}^{-1}$ .

Polyelectrolytes adsorption by the Layer-by-Layer technique onto gold electrodes or silicon wafers was performed from solutions of selected monovalent cation chlorides from Sigma-Aldrich and they were:  $\text{NH}_4\text{Cl}$ ,  $\text{LiCl}$ ,  $\text{NaCl}$ ,  $\text{KCl}$ ,  $\text{RbCl}$ ,  $\text{CsCl}$ , respectively with constant concentration of polyelectrolyte equal to 0.5 g/L and ionic strength of electrolytes equal to 0.15 M. The polyelectrolyte solutions were prepared directly before every single deposition experiment. Adsorption of any polyion layer took 10 min followed by triple rinsing for 1 min in water. The process was cycled up to 10 layer film.

### 2.2. Experimental techniques

#### 2.2.1. Quartz crystal microbalance

The quartz crystal microbalance with dissipation monitoring (QCM-D) measures the oscillation frequency of a disk-shaped piezoelectric quartz crystal with metal electrodes deposited on its both sides. In case of stiff films adsorbed on the electrodes, adsorbate induces a decrease in resonant frequency ( $\Delta f$ ), directly proportional to the mass adsorbed ( $\Delta m$ ), according to the Sauerbrey's relationship:

$$\Delta m = - \frac{C \times \Delta f}{n}$$

where  $\Delta m$  is the adsorbed mass,  $\Delta f$  is the shift in the frequency,  $C = 17.7 \text{ ng/cm}^2 \text{ Hz}$  for gold sensors applied in current studies, and  $n$  is the number of overtone used for the experiment oscillation:  $n = 1, 3, 5, 7, \dots$ . The Sauerbrey's relationship is valid only when the difference between dissipation values for measured overtones does not exceed  $10^{-6}$ . In other cases the viscoelastic models of the film need to be used to evaluate its properties as the dissipation increment ( $\Delta D$ ) is related to viscoelastic properties of adsorbed multilayers. Measurements of sequential adsorption of polyions were performed *in situ* using the QCM-D equipment by Q-Sense AB Gothenburg, Sweden (present name: Biolin Scientific). The experiments were performed at  $25^\circ \text{C}$ . The extended viscoelastic model, implemented in QTools 3 software, Q-Sense AB Gothenburg was used to calculate the experimental data.

### 2.3. Atomic force microscopy

The AFM images of “wet” polyelectrolyte films were obtained with the Dimension Icon atomic force microscope (Bruker, Santa Barbara, CA) working in the fluid in the Peak Force Tapping (PFT) mode. Standard silicon cantilevers for PFT in fluids (Bruker) with nominal spring constant of 0.7 N/m and tip radius < 10 nm were used for those measurements.

### 2.4. Cyclic voltammetry

Cyclic voltammetry (CV) measurements were conducted using Autolab rotating disk electrode and potentiostat/galvanostat (PGSTAT302N). Autolab glass cell with Pt-foil counter electrode and Ag/AgCl/sat. KCl reference electrode was used. The working electrode was rotating disk electrode (RDE) of 3 mm diameter gold disk either bare or covered by the polyelectrolyte multilayers. Experiments were performed in the equimolar  $10^{-3}$  M solution of potassium hexacyanoferrate (II) and potassium hexacyanoferrate (III) with 0.15 M NaCl as the supporting electrolyte. Third cycles of CV were selected to compare all results in the potential range of  $-0.1$  to  $+0.6$  V at the scan rate of  $50 \text{ mV s}^{-1}$ . Before measurements, all solutions were deoxidized by bubbling with laboratory grade argon (Linde Gas Poland).

## 3. Results

Quartz Crystal Microbalance with Dissipation was used to determine the masses of the adsorbed films. The results are depicted in Fig. 1. One can see differences in mass for the sequence of 1- to 10-layer PDADMAC/PSS multilayers in dependence of counter-cation applied in accordance with the following trend:  $\text{NH}_4^+ < \text{Li}^+ < \text{Na}^+ < \text{K}^+ < \text{Rb}^+ < \text{Cs}^+$ . The point size matches the experimental scatter. In case of monoatomic cations, mass of film per layer increases with the size of counter-cation. Results indicate that larger, more polarizable, chaotropic cations ( $\text{Cs}^+$ ,  $\text{Rb}^+$ ) facilitated thicker film growth, resulting in bigger mass per layer, which was seen in the whole range of studied multilayers. This suggests that larger counter-cations promote greater deposition of polyelectrolytes, possibly due to weaker hydration shells around them allowing better penetration and packing of polyelectrolyte chains. Smaller, more kosmotropic cations ( $\text{Li}^+$ ,  $\text{Na}^+$ ) lead to less mass adsorption per layer. In

case of  $\text{NH}_4^+$  one can observe an anomaly: despite its intermediate size (close to  $\text{K}^+$  size),  $\text{NH}_4^+$  used as counter-cation leads to lowest mass likely to its hydrogen-bonding capability, which may reduce its efficiency in promoting layer growth compared to alkali cations.

Voltammetric experiments were performed to investigate the permeability of the films and to (eventually) check whether this parameter can be related to the thickness of the multilayers. From data depicted in Fig. 2, one can see the decrease of maximum current in dependence on number of layers and type of polycation applied for deposition. It gives an insight into permeability and thus, the structure of obtained films. First of all, 10-layer films are less permeable than 9-layer ones. Among films of the same number of layers, the differences in maximum peak currents are clearly visible.

To improve analysis, the normalized current reduction factor (N) [33] was calculated according to formula:

$$\Delta N = (I_{\text{bare}} - I_L) / (I_{\text{bare}} - I_E), \text{ where:}$$

$I_{\text{bare}}$  is the cathodic peak current for the bare gold electrode in the solution of the electroactive probe, measured as  $I_{\text{bare}} = -0.02908$ ;

$I_L$  is the cathodic peak current for the electrode with polyelectrolyte multilayer in the solution of the electroactive probe;

$I_E$  is the cathodic current for the electrode with polyelectrolyte multilayer in the solution of pure base electrolyte at the potential of the cathodic peak observed at the bare electrode, measured as  $I_E = 0.002 \text{ mA}$ . Calculated data are collected in the Table 1.

The value of  $\Delta N$  represents the degree of electrochemical blocking by the polyelectrolyte multilayers with  $\Delta N = 0$  for fully permeable film and  $\Delta N = 1$  for completely impermeable one. All cases in between point to partial blocking. As far as 9-layer films are concerned, one can see that highest  $\Delta N$  factor and, thus, blocking exhibits in the case of films deposited in the presence of  $\text{NH}_4^+$ . Maximal current is reduced significantly ( $\Delta N = 0.733$ ), showing stronger blocking than other studied cations. The possible explanation for this is its tetrahedral structure or hydrogen-bonding capability enhancing layer stability and/or density. For other counter-cations, blocking increases from  $\text{Na}^+$  ( $\Delta N = 0.371$ ) to  $\text{K}^+$  ( $\Delta N = 0.476$ ) and then decreases slightly for  $\text{Rb}^+$  ( $\Delta N = 0.380$ ) and  $\text{Cs}^+$  ( $\Delta N = 0.376$ ). This suggests that rather specific interactions between counter-cations and polyions than size of counter-cations only are responsible for the degree of permeability. In case of 10-layer films, strongest blocking occurs also in the case of  $\text{K}^+$  ( $\Delta N = 0.907$ ), decreasing

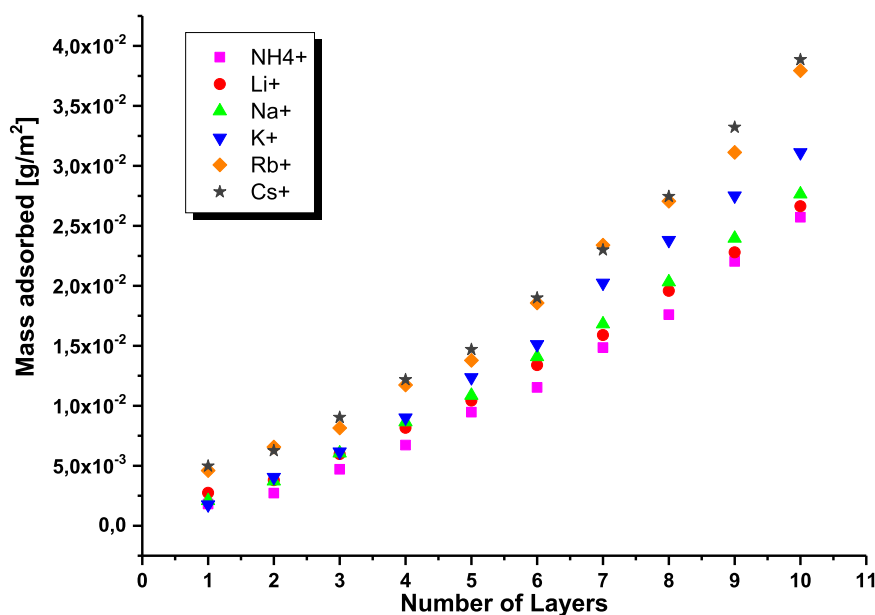
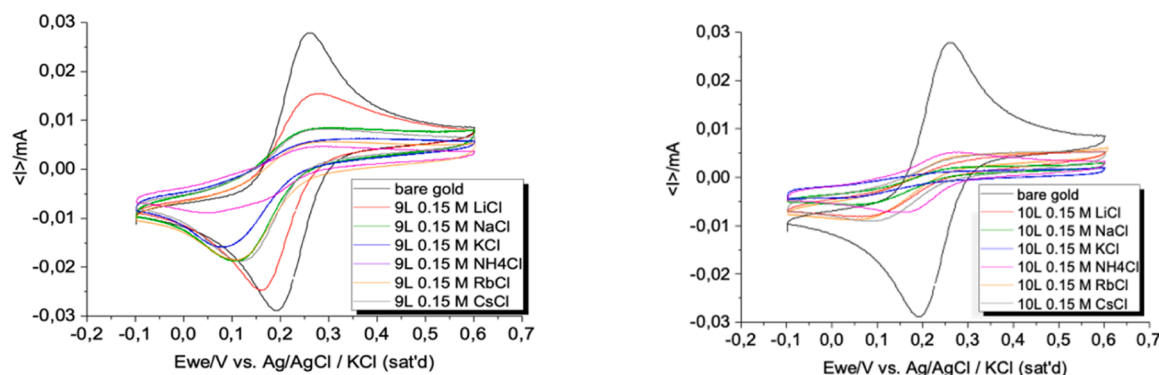


Fig. 1. Dependence of QCM-D mass of PDADMAC/PSS multilayers formed in the presence of the selected monovalent cations:  $\text{NH}_4^+ < \text{Li}^+ < \text{Na}^+ < \text{K}^+ < \text{Rb}^+ < \text{Cs}^+$ , respectively.



**Fig. 2.** Voltammograms registered for 9-layer (A) and 10-layer (B) PDADMAC/PSS multilayers formed in the presence of the selected monovalent cations:  $\text{NH}_4^+$ ,  $\text{Li}^+$ ,  $\text{Na}^+$ ,  $\text{K}^+$ ,  $\text{Rb}^+$ ,  $\text{Cs}^+$  respectively, compared with bare gold electrodes.

**Table 1**

Normalized current reduction factor,  $\Delta N$  calculated for 9-layer and 10-layer films.

Cation	9-layer film (PDADMAC/ PSS) <sub>4</sub> PDADMAC		10-layer film (PDADMAC/PSS) <sub>5</sub>	
	$I_{L,c}$ cathodic peak current electrode with PEM [mA]	$\Delta N$ , normalized current reduction factor	$I_{L,c}$ cathodic peak current electrode with PEM [mA]	$\Delta N$ , normalized current reduction factor
$\text{NH}_4^+$	-0,0092	0733	-0,0070	0815
$\text{Li}^+$	-0,0249	0154	-0,0080	0778
$\text{Na}^+$	-0,0190	0371	-0,0056	0867
$\text{K}^+$	-0,0162	0476	-0,0045	0907
$\text{Rb}^+$	-0,0188	0380	-0,0082	0771
$\text{Cs}^+$	-0,0189	0376	-0,0089	0745

for both: smaller  $\text{Li}^+$  ( $\Delta N = 0778$ )  $\text{Na}^+$  ( $\Delta N = 0867$ ) and bigger ones ( $\text{Rb}^+$  ( $N = 0771$ ) and  $\text{Cs}^+$  ( $N = 0745$ )). Multilayers with  $\text{NH}_4^+$  blocks less then films with  $\text{K}^+$  and  $\text{Na}^+$ , but more than  $\text{Rb}^+$  and  $\text{Cs}^+$ . As it was written above, its distinctive structure and chemistry may enhance layer stability and/or density in a different way than alkali, monoatomic ions.

Wetting characterization was obtained by measuring the contact angle of water on the top of the series of PDADMAC/PSS multilayers.

Results are presented in Fig. 3. The point size matches the experimental scatter. A pronounced odd–even effect in contact angle for number of layers  $> 3$  in all investigated systems reflects the nature of the outermost layer in the PEM structure. Odd-numbered films are terminated with PDADMAC, a relatively hydrophobic quaternary ammonium-based polycation, whereas even-numbered films are terminated with PSS, a more hydrophilic polyanion bearing sulfonate groups. This alternating pattern results in periodic variation in surface energy and wetting properties, with odd-numbered layers consistently exhibiting higher contact angles. The phenomenon is well-established in the literature for strong polyelectrolyte systems and is attributed to differences in hydration, surface charge, and polymer chain flexibility between the two polyelectrolytes.

One can observe that the contact angle does not strictly follow the counter-cation's size. Films deposited with  $\text{K}^+$  results in the most hydrophobic surface (highest contact angle values), while those with smaller ions ( $\text{Li}^+$ ,  $\text{Na}^+$ ) as well as larger ones ( $\text{NH}_4^+$ ,  $\text{Rb}^+$ ,  $\text{Cs}^+$ ) exhibit more hydrophilic surfaces. This suggests that the presence of  $\text{K}^+$  creates conditions for promoting a more compact or less hydrated polyelectrolyte film, reducing water interactions at the surface. The presence of other cations may disrupt this structure, allowing water to interact with the surface to a greater extent. Films with  $\text{NH}_4^+$  shows highest

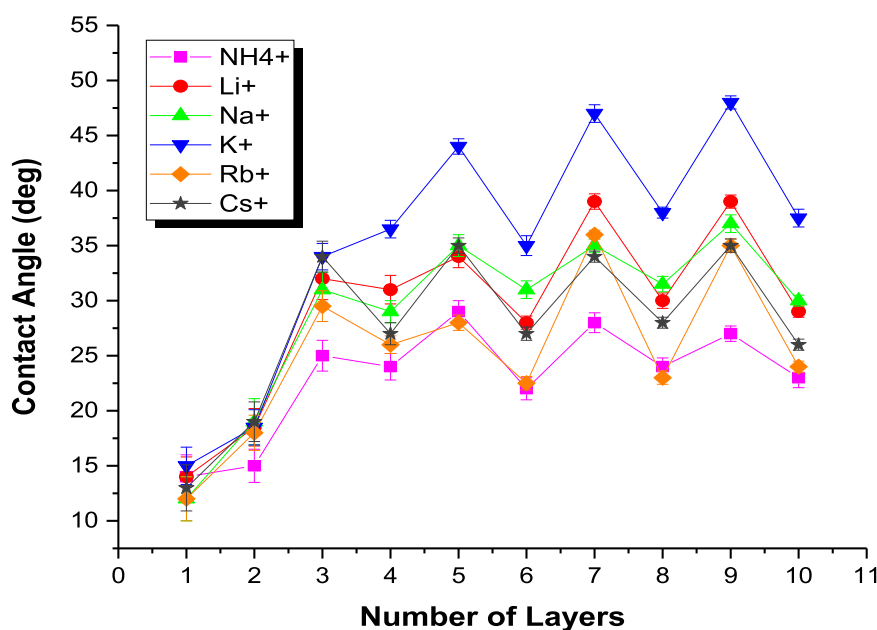


**Fig. 3.** Dependence of contact angle formed by water droplet on the surface of PDADMAC/PSS multilayers formed in the presence of the selected monovalent cations:  $\text{K}^+ > \text{Li}^+ > \text{Na}^+ > \text{Cs}^+ > \text{Rb}^+ > \text{NH}_4^+$ , respectively.

hydrophilicity probably as a result of ability of  $\text{NH}_4^+$  to form hydrogen bonds with water which enhances degree of hydrophilicity. Since  $\text{NH}_4^+$  and  $\text{K}^+$  have similar ionic sizes and show the most extreme contact angle values, it is not the ionic size which governs wetting characteristics.

Surface morphology of PDADMAC/PSS films adsorbed in the presence of  $\text{NH}_4^+$ ,  $\text{Li}^+$ ,  $\text{Na}^+$ ,  $\text{K}^+$ ,  $\text{Rb}^+$ ,  $\text{Cs}^+$  as counter-cations respectively, was studied by AFM. The AFM images, thickness profiles and root-mean-square roughness are depicted in Figs. 4 and 5.

One can see that both: root-mean-square roughness (RMS) and film thickness varied depending on the counter-cation for both types of PDADMAC/PSS films, i.e., terminated with polycation (Fig. 4) and with polyanion (Fig. 5). For all studied counter-cations, roughness is higher for 9-layer films, i.e., terminated with polycation. Larger cations ( $\text{Cs}^+$  and  $\text{Rb}^+$ ) lead to more compact, ordered films with lower RMS and higher thickness.  $\text{NH}_4^+$  and  $\text{Na}^+$  result in rougher films, indicating irregular growth.

4. Discussion

The build-up of PDADMAC/PSS polyelectrolyte multilayers, as characterized by quartz crystal microbalance (QCM-D), atomic force microscopy (AFM), cyclic voltammetry (CV), and contact angle measurements, is significantly modulated by the identity of monovalent counter-cation. Both QCM mass and AFM thickness data indicate that larger, chaotropic cations ( $\text{Cs}^+$ ,  $\text{Rb}^+$ ) facilitate thicker films with higher mass adsorption per layer and lower roughness, suggesting smoother and more compact structures. This is likely due to their weaker hydration shell and higher polarizability, which enhance charge screening and promote denser polyelectrolyte chain packing. In contrast, smaller, kosmotropic cations ( $\text{Li}^+$ ,  $\text{Na}^+$ ) result in thinner, rougher films with higher permeability, indicative of looser or more disordered growth. The anomalous behavior of  $\text{NH}_4^+$ , which yields the lowest mass deposition despite its intermediate size (comparable to  $\text{K}^+$ ), may reflect its unique

hydration dynamics driven by hydrogen-bonding capabilities, reducing polyelectrolyte adsorption efficiency. Notably, polycation-terminated (9-layer) films are consistently rougher than polyanion-terminated (10-layer) films, likely due to the more flexible conformation of PDADMAC chains compared to the rigid, aromatic backbone of PSS. For easier tracking the data, they have been collected in the Table 2.

These findings align with Hofmeister series, where ion-specific effects govern polyelectrolyte-counterion interactions, and are consistent with prior studies on ion effects in PEM systems. For instance, Salomaki et al. demonstrated that chaotropic anions (e.g.,  $\text{ClO}_4^-$ ) promoted thicker PDADMAC/PSS multilayer compared to kosmotropic anions (e.g.,  $\text{F}^-$ ), attributed to enhanced charge screening and reduced ion hydration [16, 34]. Our results extend this to cations, showing that  $\text{Cs}^+$  and  $\text{Rb}^+$  similarly enhance film thickness, while  $\text{Li}^+$  and  $\text{Na}^+$  produce thinner films, suggesting a parallel role of ion polarizability across ion types. This is comparable to findings by Haitami et al., who reported that chaotropic anions (e.g.,  $\text{ClO}_4^-$ ) produce denser, less permeable PAH/PSS films, while kosmotropic anions result in looser, more permeable structures [28]. However, the exceptional behavior of  $\text{K}^+$ , which induces high roughness, strong electrochemical blocking, and the highest hydrophobicity, deviates from a simple size-dependent trend. Our observation that  $\text{Cs}^+$  and  $\text{Rb}^+$  yield moderately permeable films, despite their thickness, contrasts with  $\text{K}^+$ 's strong blocking ( $N = 0.907$  for 10-layer films), suggesting specific interactions between  $\text{K}^+$  and PSS sulfonate groups that enhance film density. To further contextualize these results, recent studies provide additional insights into ion-specific effects. Wong et al. investigated the role of monovalent cations in PDADMAC/PSS multilayers and found that larger cations (e.g.,  $\text{Cs}^+$ ) increase film thickness and reduce swelling due to weaker hydration, consistent with our QCM and AFM data [35]. However, they noted that  $\text{K}^+$  can induce unique conformational changes in polyelectrolyte chains, potentially due to optimal ion-pairing with sulfonate groups, which may explain the high hydrophobicity and blocking efficiency observed in our

9-layer film (PDADMAC/PSS) <sub>4</sub> PDADMAC			
Type of ion thickness [nm]; RMS [nm]	Image and thickness profile	Type of ion thickness[nm] RMS [nm]	Image and thickness profile
<b>NH<sub>4</sub><sup>+</sup></b>  12.9±2.8  3.0±1.6		<b>K<sup>+</sup></b>  13.1±3.0;  4.0±1.9	
<b>Li<sup>+</sup></b>  10.6±1.4  2.8±0.8		<b>Rb<sup>+</sup></b>  13.5±1.6;  1.8±0.8	
<b>Na<sup>+</sup></b>  12.4±2.6  2.9±0.9		<b>Cs<sup>+</sup></b>  14.2±1.8;  2.4±0.6	

Fig. 4. AFM topography images and line profiles for 9-layer (positively terminated) PDADMAC/PSS<sub>4</sub>PDADMAC films deposited in the presence of  $\text{NH}_4^+$ ,  $\text{Li}^+$ ,  $\text{Na}^+$ ,  $\text{K}^+$ ,  $\text{Rb}^+$ ,  $\text{Cs}^+$  respectively, as counter-cations.



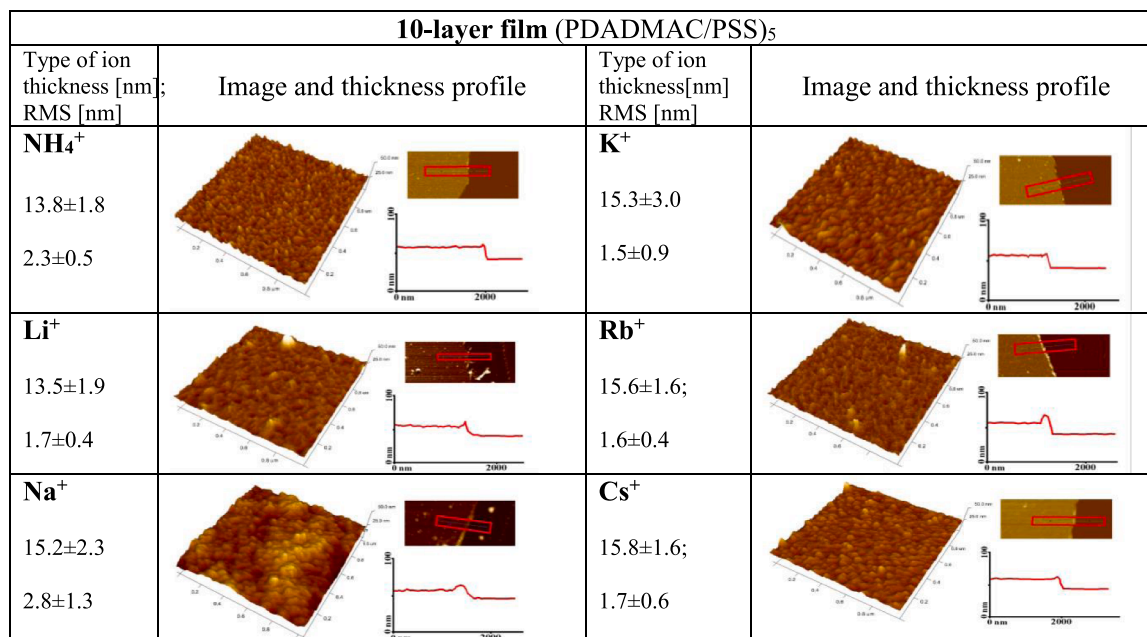


**Fig. 5.** AFM topography images and line profiles for 10-layer (negatively terminated) PDADMAC/PSS)<sub>5</sub> films deposited in the presence of NH<sub>4</sub><sup>+</sup>, Li<sup>+</sup>, Na<sup>+</sup>, K<sup>+</sup>, Rb<sup>+</sup>, Cs<sup>+</sup> as counteranions.

**Table 2**

AFM RMS roughness and thickness and QCM mass for all studied samples of PDADMAC/PSS films deposited in the presence of NH<sub>4</sub><sup>+</sup>, Li<sup>+</sup>, Na<sup>+</sup>, K<sup>+</sup>, Rb<sup>+</sup>, Cs<sup>+</sup> as counteranions.

Cation	9-layer film			10-layer film		
	RMS [nm]	thickness [nm]	QCM mass [g/m <sup>2</sup> * 10 <sup>-2</sup> ]	RMS [nm]	thickness [nm]	QCM mass [g/m <sup>2</sup> * 10 <sup>-2</sup> ]
NH <sub>4</sub> <sup>+</sup>	3.0 ± 1.6	12.9 ± 2.8	2.2 ± 0.3	2.3 ± 0.5	13.8 ± 1.8	2.6 ± 0.2
Li <sup>+</sup>	2.8 ± 0.8	10.6 ± 1.4	2.3 ± 0.4	1.7 ± 0.4	13.5 ± 1.9	2.7 ± 0.3
Na <sup>+</sup>	2.9 ± 0.9	12.4 ± 2.6	2.4 ± 0.2	2.8 ± 1.3	15.2 ± 2.3	2.8 ± 0.3
K <sup>+</sup>	4.0 ± 1.9	13.1 ± 3.0	2.8 ± 0.4	1.5 ± 0.9	15.3 ± 3.0	3.1 ± 0.2
Rb <sup>+</sup>	1.8 ± 0.8	13.5 ± 1.6	3.1 ± 0.2	1.6 ± 0.4	15.6 ± 1.6	3.7 ± 0.2
Cs <sup>+</sup>	2.4 ± 0.6	14.2 ± 1.8	3.3 ± 0.3	1.7 ± 0.6	15.8 ± 1.6	3.9 ± 0.1

K<sup>+</sup>-deposited films. Similarly, Wang et al. explored cation effects on polyelectrolyte brushes and reported that chaotropic cations maintain extended, hydrated conformations [36]. This supports our finding that Cs<sup>+</sup> and Rb<sup>+</sup> produce compact films while Li<sup>+</sup> and Na<sup>+</sup> result in looser, more permeable structures. The distinct behavior of NH<sub>4</sub><sup>+</sup>, which leads to the lowest mass and highest hydrophilicity, aligns with Kou et al., who highlighted NH<sub>4</sub><sup>+</sup>'s deviation from the Hofmeister series due to its hydrogen-bonding capacity, affecting polyelectrolyte interactions differently than alkali cations [20]. Zhang and Cremer further noted that NH<sub>4</sub><sup>+</sup>'s hydrogen-bonding enhances water interactions, which may explain the hydrophilic surfaces observed in our NH<sub>4</sub><sup>+</sup>-deposited films [24]. The permeability results, assessed via the normalized current reduction factor (N), corroborate the structural findings. Thicker films formed with chaotropic cations (Cs<sup>+</sup>, Rb<sup>+</sup>) exhibit moderate blocking suggesting a dense barrier to redox probe diffusion, while thinner films with kosmotropic cations (Li<sup>+</sup>, Na<sup>+</sup>) are more permeable. The strong blocking by K<sup>+</sup>-deposited films, despite their high roughness, indicates a heterogeneous yet tightly packed structure. This is intriguing when

compared to Elzbieciak-Wodka et al., who found that divalent cations (e.g., Mg<sup>2+</sup>) significantly reduce PEM permeability due to stronger electrostatic cross-linking [27]. While monovalent cations in our study do not achieve such cross-linking, K<sup>+</sup>'s behavior suggests specific ion-polyelectrolyte interactions, possibly ion-pairing, as proposed by Gregory et al. for Hofmeister effects in polyelectrolyte systems [22]. The high hydrophobicity of K<sup>+</sup>-deposited films, evidenced by the highest contact angles, further supports a compact, less hydrated surface, consistent with Dressick et al., who linked ion-specific effects to altered surface energy in PEMs [26]. The pronounced odd-even effect in contact angle, driven by alternating PDADMAC (more hydrophobic) and PSS (more hydrophilic) terminated layers, is well established in strong polyelectrolyte systems. Our results align with Schlenoff et al., who attributed this alternation to differences in surface charge, hydration, and chain flexibility [25]. The higher roughness of PDADMAC-terminated films may reflect the flexibility of PDADMAC chains, as noted by Tang and Besseling, who linked polyelectrolyte chain dynamics to multilayer morphology under varying ionic conditions [14]. The hydrophilic nature of NH<sub>4</sub><sup>+</sup>-deposited films likely stems from enhanced water interactions, as supported by Chituru et al., who emphasized the role of non-electrostatic interactions (e.g., hydrogen bonding) in polyelectrolyte complexes [23].

In comparison to the broader literature, our study underscores the complexity of ion-specific effects, where cation size, hydration, and chemical interactions interplay to govern PEM properties. The trend of thicker, smoother films with chaotropic cations (Cs<sup>+</sup>, Rb<sup>+</sup>) and thinner, rougher films with kosmotropic cations (Li<sup>+</sup>, Na<sup>+</sup>) is consistent with established Hofmeister effects, as seen in [16,35]. However, the deviations of K<sup>+</sup> and NH<sub>4</sub><sup>+</sup> highlight the need to consider specific ion-polyelectrolyte interactions beyond simple size or hydration models. The strong blocking and hydrophobicity of K<sup>+</sup>-deposited films suggest potential applications in electrochemical sensors or antifouling coatings, where controlled permeability and surface energy are critical. Similarly, the high permeability of Li<sup>+</sup> and Na<sup>+</sup>-deposited films could be leveraged for selective transport membranes. These findings build on prior work, such as [35,36], by providing a systematic analysis of monovalent cation effects on PDADMAC/PSS multilayers, offering new insights into tailoring PEM properties through ion selections. Future studies could employ molecular dynamics simulations or spectroscopic techniques to

elucidate the mechanisms underlying  $K^+$ 's unique effects, further advancing the rational design of functional PEMs.

## 5. Conclusions

Presented research showed that larger cations ( $Rb^+$ ,  $Cs^+$ ) used for PDADMAC/PSS deposition enhance film growth and smoothness, leading to thicker but moderately permeable multilayers.  $K^+$  stands out with a denser, rougher structure, correlated with high blocking and hydrophobicity.  $NH_4^+$  unusual behavior highlights the role of hydrogen bonding in tuning film properties. Thus, linking mass deposition, film thickness and surface morphology to the wettability and electrochemical blocking leads to the conclusions that these properties of films interplay in modulating multilayer characteristics. These findings underscore how counter-cation hydration and size govern the structural and functional characteristics of polyelectrolyte multilayers with implications for tailoring their properties in applications like sensors or coatings.

## CRediT authorship contribution statement

**Piotr Warszynski:** Supervision, Conceptualization. **Michał Szwarzynski:** Visualization, Validation, Investigation. **Magdalena Włoddek:** Visualization, Validation, Investigation. **Marta Kolasinska-Sojka:** Writing – review & editing, Writing – original draft, Visualization, Validation, Software, Formal analysis, Data curation, Conceptualization, Supervision, Resources, Project administration, Methodology, Investigation, Funding acquisition.

## Funding

This research was funded by the National Science Centre, Poland, Contract No. UMO-2016/23/B/ST8/03128.

## Declaration of Competing Interest

The authors declare that they have no known competing financial interests or personal relationships that could have appeared to influence the work reported in this paper.

## Acknowledgment

Piotr Skowron is acknowledged for conducting part of electrochemical experiments.

## Data availability

Data will be made available on request.

## References

- [1] G. Decher, Fuzzy Nanoassemblies: Toward Layered Polymeric Multicomposites Science, 277 (1997), pp. 1232–1237 DOI: [10.1126/science.277.5330.1232](https://doi.org/10.1126/science.277.5330.1232).
- [2] J.J. Richardson, J. Cui, M. Bjornmalm, J.A. Braunger, H. Ejima, F. Caruso, Innovation in layer-by-layer assembly, Chem. Rev. 116 (2016) 14828–14867, <https://doi.org/10.1021/acs.chemrev.6b00627>.
- [3] G. Decher, J.B. Schlenoff, Multilayer Thin Films: Sequential Assembly of Nanocomposite Materials, Second Edition, Wiley-VCH Verlag GmbH & Co. KGaA, 2012.
- [4] Z. Tang, Y. Wang, P. Podsiadlo, N.A. Kotov, Biomedical applications of layer-by-layer assembly: from biomimetics to tissue engineering, Adv. Mater. 18 (2006) 3203–3224, <https://doi.org/10.1002/adma.200600113>.
- [5] F. Caruso, Nanoengineering of particle surfaces, Adv. Mater. 13 (2001) 11–22, [https://doi.org/10.1002/1521-4095\(200101\)13:1<11::AID-ADMA11>3.0.CO;2-N](https://doi.org/10.1002/1521-4095(200101)13:1<11::AID-ADMA11>3.0.CO;2-N).
- [6] J.A. Regenspur, W.A. Jonkers, M.A. Junker, I. Achterhuis, E. te Brinke, W.M. de Vos, Polyelectrolyte multilayer membranes: an experimental review, Desalination 583 (2024) 117693–117707, <https://doi.org/10.1016/j.desal.2024.117693>.
- [7] L.-M. Petrila, F. Bucatariu, M. Mihai, C. Teodosiu, Polyelectrolyte multilayers: an overview on fabrication, properties, and biomedical and environmental applications, Materials 14 (2021) 4152–4181, <https://doi.org/10.3390/ma14154152>.
- [8] J.J. Richardson, M. Bjornmalm, F. Caruso, Multilayer assembly. Technology-driven layer-by-layer assembly of nanofilms, pp. aaa2491-1 - aaa2491-11, Science 348 (2015), <https://doi.org/10.1126/science.aaa2491>.
- [9] D.O. Grigoriev, T. Bukreeva, H. Mohwald, D.G. Shchukin, New method for fabrication of loaded micro- and nanocontainers: emulsion encapsulation by polyelectrolyte layer-by-layer deposition on the liquid core, Langmuir 24 (2008) 999–1004, <https://doi.org/10.1021/la702873f>.
- [10] L. Seon, P. Lavalle, P. Schaaf, F. Boulmedais, Polyelectrolyte multilayers: a versatile tool for preparing antimicrobial coatings, Langmuir 31 (2015) 12856–12872, <https://doi.org/10.1021/acs.langmuir.5b02768>.
- [11] K. Ariga, J.P. Hill, Q. Ji, Layer-by-layer assembly as a versatile bottom-up nanofabrication technique for exploratory research and realistic application, Phys. Chem. Chem. Phys. 9 (2007) 2319–2340, <https://doi.org/10.1039/B700410A>.
- [12] K. Ariga, Y. Lvov, G. Decher, There is still plenty of room for layer-by-layer assembly for constructing nanoarchitectonics-based materials and devices, Phys. Chem. Chem. Phys. 24 (2022) 4097–4115.
- [13] Marta Kolasinska, Rumen Krastev, Piotr Warszynski, Characteristics of polyelectrolyte multilayers: effect of PEI anchoring layer and posttreatment after deposition, J. Colloid Interface Sci. 305 (2007) 46–56, <https://doi.org/10.1016/j.jcis.2006.09.035>.
- [14] K. Tang, N.A.M. Besseling, Formation of polyelectrolyte multilayers: ionic strengths and growth regimes, Soft Matter 12 (2016) 1032–1040, <https://doi.org/10.1039/C5SM02118A>.
- [15] Z. Adamczyk, M. Zembala, M. Kolasinska, P. Warszynski, Characterization of polyelectrolyte multilayers on mica and oxidized titanium by streaming potential and wetting angle measurements, Colloids Surf. A Physicochem. Eng. Asp. 302 (2007) 455–460, <https://doi.org/10.1016/j.colsurfa.2007.03.013>.
- [16] M. Salomäki, P. Tervasmäki, S. Areva, J. Kankare, The Hofmeister anion effect and the growth of polyelectrolyte multilayers, Langmuir 20 (2004) 3679–3683, <https://doi.org/10.1021/la036328y>.
- [17] M. Salomäki, T. Laiho, J. Kankare, Counteranion-controlled properties of polyelectrolyte multilayers, Macromolecules 37 (2004) 9585–9590, <https://doi.org/10.1021/ma048701u>.
- [18] W. Kunz, P.L. Nostro, B.W. Ninham, The present state of affairs with Hofmeister effects, Curr. Opin. Colloid Interface Sci. 9 (2004) 1–18, <https://doi.org/10.1016/j.cocis.2004.05.004>.
- [19] W. Kunz, J. Henle, B.W. Ninham, Zur Lehre von der Wirkung der Salze (about the science of the effect of salts): Franz Hofmeister's historical papers, Curr. Opin. Colloid Interface Sci. 9 (2004) 19–37, <https://doi.org/10.1016/j.cocis.2004.05.005>.
- [20] R. Kou, J. Zhang, T. Wang, G. Liu, Interactions between polyelectrolyte brushes and Hofmeister ions: chaotropes versus kosmotropes, Langmuir 31 (2015) 10461–10468, <https://doi.org/10.1021/acs.langmuir.5b02698>.
- [21] Z. Luo, X. Wang, G. Zhang, Ion-specific effect on dynamics of polyelectrolyte chains, Phys. Chem. Chem. Phys. 19 (2012) 6812–6816.
- [22] K.P. Gregory, G.R. Elliott, H. Robertson, A. Kumar, E.J. Wanless, G.B. Webber, V.S. J. Craig, G.G. Andersson, A.J. Page, Understanding specific ion effects and the Hofmeister series, pp. 12682–12718, Phys. Chem. Chem. Phys. 24 (2022), <https://doi.org/10.1039/D2CP00847E>.
- [23] S.V. Chituru, S. Das, S. Majumdar, Impact of specific ion effects and electrostatic interactions on a polyelectrolyte-polyampholyte complex, Discov. Chem. Eng. 4 (2024) 1–12, <https://doi.org/10.1007/s43938-024-00043-y>.
- [24] Y. Zhang, P.S. Cremer, Interactions between macromolecules and ions: the Hofmeister series, Curr. Opin. Chem. Biol. 10 (2007) 658–663, <https://doi.org/10.1016/j.cbpa.2006.09.020>.
- [25] J.B. Schlenoff, H. Ly, M. Li, Charge and mass balance in polyelectrolyte multilayers, J. Am. Chem. Soc. 120 (1998) 7626–7634, <https://doi.org/10.1021/ja980350+>.
- [26] W.J. Dressick, K.J. Wahl, N.D. Bassim, R.M. Stroud, D.Y. Petrovyk, Divalent–anion salt effects in polyelectrolyte multilayer depositions (dx.doi.org/), Langmuir 28 (2012) 15831–15843, <https://doi.org/10.1021/la3033176>.
- [27] M. Elżbieciak-Wodka, M. Kolasinska-Sojka, P. Warszynski, Effect of mono- and divalent ions on the formation and permeability of polyelectrolyte multilayer films, J. Electrochem. Chem. 789 (2017) 123–132, <https://doi.org/10.1016/j.jelechem.2017.02.02>, 4.
- [28] A.E. El Haitami, D. Martel, V. Ball, H.C. Nguyen, E. Gonthier, P. Labbe, J.-C. Voegel, P. Schaaf, B. Senger, F. Boulmedais, Effect of the supporting electrolyte anion on the thickness of PSS/PAH multilayer films and on their permeability to an electroactive probe, Langmuir 25 (2009) 2282–2289, <https://doi.org/10.1021/la803534y>.
- [29] T. Kruk, K. Chojnacka-Góra, M. Kolasinska-Sojka, S. Zapotoczny, Stimuli-responsive polyelectrolyte multilayer films and microcapsules, Adv. Colloid Interface Sci. 310 (2022) 102773–102802, <https://doi.org/10.1016/j.cis.2022.102773>.
- [30] M. Szuwarzynski, K. Wolski, T. Kruk, S. Zapotoczny, Macromolecular strategies for transporting electrons and excitation energy in ordered polymer layers, Prog. Polym. Sci. 121 (2021) 101433–101474, <https://doi.org/10.1016/j.progpolymsci.2021.101433>.
- [31] W. Lijuan, W. Long, Z. Lanlan, W. Zhiqiang, A. Elbaz, Z. Qianqian, S. Quanping, Z. Yanxi, C. Fengyuan, Biocompatibility polyelectrolyte coating with water-enabled self-healing ability, J. Taiwan Inst. Chem. Eng. 91 (2018) 130–137, <https://doi.org/10.1016/j.jtice.2018.06.009>.

- [32] K.-D. Kreuer, G. Portale, A critical revision of the nano-morphology of proton conducting ionomers and polyelectrolytes for fuel cell applications, *Adv. Funct. Mater.* 23 (2013) 5390–5397, <https://doi.org/10.1002/adfm.201300376>.
- [33] M. Elzbieciak-Wodka, P. Warszynski, Effect of deposition conditions on thickness and permeability of the multilayer films formed from natural polyelectrolytes, *Electrochim. Acta* 104 (2013) 348–357, <https://doi.org/10.1016/j.electacta.2012.10.169>.
- [34] M. Salomäki, J. Kankare, Specific anion effect in swelling of polyelectrolyte multilayers, *Macromolecules* 41 (2008) 4423–4428, <https://doi.org/10.1021/ma800315j>.
- [35] J. Wong, H. Zastrow, W. Jaeger, R. von Klitzing, Specific ion versus electrostatic effects on the construction of polyelectrolyte multilayers, *Langmuir* 25 (2009) 14061–14070, <https://doi.org/10.1021/la901673u>.
- [36] T. Wang, Y. Long, L. Liu, X. Wang, V. Craig, G. Zhang, G. Liu, Cation-specific conformational behavior of polyelectrolyte brushes: from aqueous to nonaqueous solvent, *Langmuir* 30 (2014) 12850–12859, <https://doi.org/10.1021/la5033493>.